Journal of Sound and Vibration 329 (2010) 768–785

Contents lists available at ScienceDirect

Journal of Sound and Vibration

journal homepage: www.elsevier.com/locate/jsvi

Output-only identification and dynamic analysis of time-varying mechanical structures under random excitation: A comparative assessment of parametric methods

M.D. Spiridonakos, A.G. Poulimenos, S.D. Fassois *

Stochastic Mechanical Systems & Automation (SMSA) Laboratory, Department of Mechanical & Aeronautical Engineering, University of Patras, GR 265 00 Patras, Greece

ARTICLE INFO

Article history:
Received 19 October 2008
Received in revised form
3 September 2009
Accepted 5 October 2009
Handling Editor: K. Shin
Available online 4 November 2009

ABSTRACT

This article addresses the problem of parametric time-domain identification and dynamic analysis for *time-varying* (TV) mechanical structures under unobservable random excitation. The methods presented are based on time-dependent autoregressive moving average (TARMA) models, and are classified according to the mathematical structure imposed on the TV parameter evolution as unstructured parameter evolution, stochastic parameter evolution, and deterministic parameter evolution. The features and relative merits of each class are outlined. A representative method from each is then assessed through its application to the identification and dynamic analysis of a laboratory TV structure consisting of a beam with a mass moving on it. The results are mutually compared and contrasted to those obtained through "frozen-configuration" (multiple experiment) baseline identification.

Important Conventions and Symbols

Bold-face upper/lower case symbols designate matrix/column-vector quantities, respectively.

Matrix transposition is indicated by the superscript T.

A functional argument in parentheses designates function of a real variable; for instance $x(t)$ is a function of analog time $t \in \Re$.

A functional argument in brackets designates function of an integer variable; for instance $x[t]$ is a function of normalized discrete time ($t = 1, 2, \ldots$). The conversion from discrete normalized time to analog time is based on $(t-1)T_s$, with T_s standing for the sampling period.

A time instant used as superscript to a function indicates the set of values of the function up to that time instant; for instance $x^t \triangleq \{x[i], i = 1, 2, \ldots, t\}$.

A hat designates estimator/estimate of the indicated quantity; for instance $\hat{\boldsymbol{\theta}}$ is an estimator/estimate of $\boldsymbol{\theta}$.

Abbreviations: 2SLS, two stage least squares (method); APD, aggregate parameter deviation; AR, autoregressive; ARMA, autoregressive moving average; BIC, Bayesian information criterion; ELS, extended least squares; FS-TAR, functional series TAR (model); FS-TARMA, functional series TARMA (model); KF, Kalman filter; LMS, linear multi stage (method); MA, moving average; ML, maximum likelihood (method); NID, normally independently distributed; ODE, ordinary differential equation; OLS, ordinary least squares; P-A, polynomial-algebraic (method); PSD, power spectral density; RML, recursive maximum likelihood (method); RSS, residual sum of squares; SP-TARMA, smoothness priors TARMA (model); STFT, short-time Fourier transform; TAR, time-dependent AR (model); TARMA, time-dependent ARMA (model); TV, time-varying (model); TI, time-invariant (model); UPE-TARMA, unstructured parameter evolution TARMA (model).

* Corresponding author. Tel./fax: +30 2610 969495 (direct); +30 2610 969492 (central).
E-mail address: fassois@mech.upatras.gr (S.D. Fassois).
URL: http://www.smsa.upatras.gr

0022-460X/$ - see front matter © 2009 Elsevier Ltd. All rights reserved.
doi:10.1016/j.jsv.2009.10.005

Nomenclature

$a_i[t]$, $c_i[t]$	AR, MA time-dependent parameters
$\boldsymbol{a}$, $\boldsymbol{c}$, $\boldsymbol{s}$	AR, MA, innovations variance projection coefficient vectors (FS-TARMA models)
$A[\mathcal{B},t]$, $C[\mathcal{B},t]$	AR, MA time-dependent polynomial operators
$\mathcal{B}$	backshift operator ($\mathcal{B}^k x[t] \triangleq x[t-k]$)
$e[t]$	model innovations sequence
$\mathcal{F}$	functional space
$G_j[t]$	j-th basis function
n_a, n_c	AR, MA model orders
N	signal length in samples
p_a, p_c, p_s	AR, MA, innovations variance functional subspace dimensionality (FS-TARMA models)
$S(\omega,t)$	time-dependent power spectral density
T_s	sampling period
$x[t]$	vibration signal (discrete time)
$x(t)$	vibration signal (continuous time)
x^N	data set ($x[t];\ t=1,2,\ldots,N$)

Greek symbols

$\zeta_i[t]$	time-dependent i-th damping ratio
$\boldsymbol{\theta}[t]$	AR/MA parameter vector at time t
$\boldsymbol{\theta}^t$	set of AR/MA parameter vectors at times $1,\ldots,t$
$\boldsymbol{\vartheta}$	AR/MA projection coefficient vector (FS-TARMA models)
κ	constraint equation order (SP-TARMA models)
λ	forgetting factor (UPE-TARMA models)
$\sigma_e^2[t]$	innovations sequence variance
$\omega_{n_i}[t]$	time-dependent i-th natural frequency in rad/s

1. Introduction

Time-varying (TV), or else *nonstationary*, mechanical structures are those characterized by (mass, stiffness, power dissipation) properties that vary with time. Prime examples include crane and similar structures, robotic and other variable configuration structures, railway bridges, rocket and aircraft structures, rotating structures, vehicle suspensions with adjustable characteristics, deployable space structures, and so on. *Continuously variable configuration* structures, that is structures with geometrical characteristics varying with time, constitute an important subclass of TV structures.

TV structures are often subject to random excitation producing random vibration responses. In contrast to time-invariant (TI) structures which produce vibration responses with TI (*stationary*) statistical characteristics, the responses of TV structures are characterized by TV (*nonstationary*) statistical characteristics [1, Ch. 12, 2–6]. Nonstationary responses may be also produced by TI structures subject to nonstationary excitation (such as earthquakes and atmospheric turbulence), or by structures with inherent nonlinear dynamics. Although these cases may be also treated by the methods of this article, our main focus will be on TV structures.

In many cases it is useful to identify a model of a TV structure which may be subsequently used for dynamic analysis [7–11], for the refinement of analytical models [12], for simulation [13], for damage detection and identification [14–16], as well as for prediction and control [17]. Oftentimes, this identification has to be based on vibration response-only measurements (the *output-only problem*). This is so because the force excitation may be due to various sources that are difficult or impossible to precisely isolate and measure (this is the case of oscillations in a crane system, a rocket, a railway bridge, and so on). The focus of this article is precisely on this case, although the methods may be extended to the observable excitation case as well (for instance see [12,15,18]). A recent survey on the topic is Ref. [2], where the methods surveyed are compared by means of a Monte Carlo study based on a TV suspension model.

The mathematical models for the output-only identification of TV structures may be of the *parametric* or *nonparametric* types. Attention is presently restricted to the former category, which is known to offer a number of potential advantages compared to the category of nonparametric methods [2,5,7,8]. These include (i) representation parsimony, (ii) improved accuracy, (iii) improved frequency resolution, (iv) improved tracking of the time-varying dynamics, and (v) flexibility in analysis, as parametric methods are capable of directly capturing the underlying dynamics responsible for the time-varying behavior. The reader may consult references such as [5,19,20] for nonparametric methods.

Parametric mathematical models are of the time-dependent autoregressive moving average (TARMA) type or corresponding state space forms [10]. TARMA models resemble their conventional, stationary ARMA counterparts [21, p. 53], with the significant difference being that they allow their parameters to depend on time [2,8,22–25]. Depending on the nature of the mathematical structure imposed on the time evolution of their parameters, TARMA models may be classified as unstructured parameter evolution, stochastic parameter evolution, and deterministic parameter evolution.

Unstructured parameter evolution TARMA (UPE-TARMA) models impose no mathematical structure on the time evolution of their parameters, which are thus free to change with time. Such a model is thus directly parameterized in terms of its TV parameters. As the complete description of a TV structure requires knowledge of the model parameters at each time instant, UPE-TARMA models are characterized by low parsimony (low model parametrization economy) and are mainly capable of tracking slow evolutions in the dynamics. Due to their simplicity and ease of use, they are frequently used in practice (for instance see [24–27]).

The class of stochastic parameter evolution TARMA models impose stochastic structure on the time evolution of their parameters. The latter are thus assumed to be autocorrelated random variables allowed to change with time, but with their

evolution being subject to certain smoothness constraints. These are often referred to as *smoothness priors constraints*, and the models are thus referred to as *smoothness priors TARMA* (SP-TARMA) models. SP-TARMA models achieve low parsimony, as knowledge of the model parameters at each time instant is still required. At the same time, they may still leave an unnecessarily high number of degrees of freedom in parameter evolution. SP-TARMA models have been used primarily for the modelling and analysis of earthquake ground motion signals (for instance see [6,28,29]).

Finally, deterministic parameter evolution TARMA models impose deterministic structure on the time evolution of their parameters. This is achieved by postulating model parameters as deterministic functions of time belonging to specific *functional subspaces* [2,7,14,22, Chapter 6,23,30]. These models are specifically referred to as *functional series TARMA* (FS-TARMA) models. FS-TARMA models achieve high parsimony, as they use a limited number of parameters. Through proper selection of the functional subspaces, FS-TARMA models may represent various types of evolution in the dynamics, including slow, fast or even discontinuous evolutions [7,8,13,17,22, p. 215, 31].

FS-TAR/TARMA models have been used in various structural dynamics related applications, such as the modelling and simulation of earthquake ground motion [13,32], vibration analysis in rotating machinery [7], the modelling and prediction of power consumption in an automobile active suspension [17], the modelling and analysis of simulated robot vibration [8], and the modelling and vibration analysis of a bridge with heavy vehicle type laboratory structure [11].

The aim of the present study is twofold: (i) to provide a concise overview of the techniques of time-dependent ARMA methods for TV structural identification and (ii) to present an application and comparative assessment of the methods through a case study, pertaining to the modelling and dynamic analysis of the nonstationary random vibration of a time-varying bridge with heavy vehicle type laboratory structure. Comparisons with a "frozen-configuration" baseline model based on multiple stationary experiments are also made.

The remainder of this paper is organized as follows: the mathematical description of a TV and a continuously variable configuration structure and their connection are discussed in Section 2. The parametric models for the output-only identification of TV structures are presented in Section 3, while in Section 4 the model parameter estimation and model structure selection problems are considered. In Section 5 the TV (continuously variable configuration) structure under study is presented. The identification results and the dynamic analysis of the structure based on the identified TARMA models are in the focus of Sections 6 and 7, respectively. Finally the conclusions of the study are summarized in Section 8.

2. Time-varying and continuously variable configuration structures and their response

A lumped parameter model of a TV viscously damped structure is provided by the ordinary differential equation (ODE)

$$\boldsymbol{M}(t)\ddot{\boldsymbol{x}}(t)+\boldsymbol{C}(t)\dot{\boldsymbol{x}}(t)+\boldsymbol{K}(t)\boldsymbol{x}(t)=\boldsymbol{f}(t),\quad t\in[t_0,t_f] \tag{1}$$

with t designating analog time, $\boldsymbol{x}(t)$ the structural displacement response vector, and $\boldsymbol{f}(t)$ the force excitation vector. $\boldsymbol{M}(t)$, $\boldsymbol{C}(t)$, and $\boldsymbol{K}(t)$ stand for the TV mass, viscous damping, and stiffness matrices, respectively, which are responsible for the TV nature of the structure.

By "freezing" the mass, viscous damping, and stiffness matrices successively at each time instant τ ($\tau\in[t_0,t_f]$), one may associate a noncountable sequence of TI structures with the TV structure of Eq. (1). Each such *"frozen" structure* is described by the ODE

$$\boldsymbol{M}(\tau)\ddot{\boldsymbol{x}}(t)+\boldsymbol{C}(\tau)\dot{\boldsymbol{x}}(t)+\boldsymbol{K}(\tau)\boldsymbol{x}(t)=\boldsymbol{f}(t)\quad\text{for all } t \tag{2}$$

which is TI for the selected time instant τ. This sequence of TI structures may be thought of as a "*frozen-time*" *representation* of the TV structure. The knowledge of the frozen-time representation of a TV structure is equivalent to knowledge of the TV structure and vice versa, as it provides the characteristics that the structure would have if it were indeed frozen at each time instant.

As already noted, continuously variable configuration structures characterized by geometrical characteristics that vary with time, form an important subclass of TV structures. Defining a *configuration vector* $\boldsymbol{r}(t)$ that fully describes the geometry of the continuously variable configuration structure at each time instant, the structure matrices of Eq. (1) become functions of $\boldsymbol{r}(t)$, that is $\boldsymbol{M}(t)\equiv\boldsymbol{M}(\boldsymbol{r}(t))$, $\boldsymbol{C}(t)\equiv\boldsymbol{C}(\boldsymbol{r}(t))$, and $\boldsymbol{K}(t)\equiv\boldsymbol{K}(\boldsymbol{r}(t))$.

By analogy to the frozen-time representation of a TV structure, the "*frozen-configuration*" *representation* of a continuously variable configuration structure may be thought of as consisting of a noncountable sequence of TI structures obtained by "freezing" the configuration vector successively at each time instant τ ($\tau\in[t_0,t_f]$). Designating the frozen-configuration vector $\boldsymbol{r}(\tau)=\boldsymbol{\rho}$, each such frozen structure is described by the ODE

$$\boldsymbol{M}(\boldsymbol{\rho})\ddot{\boldsymbol{x}}(t)+\boldsymbol{C}(\boldsymbol{\rho})\dot{\boldsymbol{x}}(t)+\boldsymbol{K}(\boldsymbol{\rho})\boldsymbol{x}(t)=\boldsymbol{f}(t)\quad\text{for all } t \tag{3}$$

and is TI for the selected $\boldsymbol{\rho}$. Obviously, the frozen-time and frozen-configuration representations are equivalent for a continuously variable configuration structure with known time variation of its configuration vector.

A practically important feature of continuously variable configuration structures is that it is often possible to obtain access to a (configuration-vector-discretized) version of its frozen-configuration representation by "freezing" the configuration vector at selected discrete values (say $\boldsymbol{\rho}_1,\boldsymbol{\rho}_2,\ldots,\boldsymbol{\rho}_M$). The dynamics of the structure for each value of $\boldsymbol{\rho}$ are described by Eq. (3), and identification of its frozen-configuration representation may be based on data sets obtained from M distinct experiments. This procedure is referred to as *baseline identification* and is used in the present article as well.

Its advantage is twofold: conventional TI identification is used, and the achievable accuracy may be high due to the availability of (large) data sets from M experiments. Yet, its disadvantage is exactly the need for running M distinct experiments and identification cycles. Moreover, TI identification does not directly provide information on the actual nonstationary vibration response.

The above concepts and ideas obviously extend to the discrete-time case. The ODE representation of Eq. (1) is then converted into a vector second-order difference equation. When the single excitation single vibration response is considered, the (partial) dynamics may be described by a scalar difference equation

$$x[t]+\sum_{i=1}^{n_a} a_i[t]x[t-i]=\sum_{i=0}^{n_c} c_i[t]f[t-i], \quad t=1,\ldots,N \tag{4}$$

in which t designates normalized discrete-time (absolute time normalized by the sampling period), $f[t]$, $x[t]$ the discretized versions of the scalar force and observed vibration displacement response, respectively, $a_i[t]$, $c_i[t]$ the discrete-time TV parameters, n_a, n_c the equation orders, and N the signals' length in samples. The expressions for the discrete-time frozen-time and frozen-configuration representations are analogous to their continuous-time counterparts.

3. Parametric models for the identification of time-varying structures

Parametric models typically are of the TARMA type or proper extensions (for instance TARMAX models—that is TARMA models with exogenous excitation, which additionally account for measurable force excitations). A TARMA(n_a, n_c) model, with n_a, n_c designating its autoregressive (AR) and moving average (MA) orders, respectively, is thus of the form [compare with Eq. (4)]

$$\underbrace{x[t]+\sum_{i=1}^{n_a} a_i[t]x[t-i]}_{\text{AR part}}=\underbrace{e[t]+\sum_{i=1}^{n_c} c_i[t]e[t-i]}_{\text{MA part}}, \quad e[t]\sim\text{NID}(0,\sigma_e^2[t]) \tag{5}$$

with t designating normalized discrete time, $x[t]$ the nonstationary vibration response signal, $e[t]$ an unobservable uncorrelated (white) nonstationary *innovations*, or else *residual* signal characterized by zero mean and TV variance $\sigma_e^2[t]$, and $a_i[t]$, $c_i[t]$ the model's TV AR and MA parameters, respectively. NID$(\cdot,\cdot)$ stands for normally independently distributed random variables with the indicated mean and variance.

As already indicated, depending on the nature of the mathematical structure imposed on the time evolution of their parameters, TARMA models may be classified as unstructured parameter evolution, stochastic parameter evolution, and deterministic parameter evolution.

3.1. Unstructured parameter evolution TARMA models

Unstructured parameter evolution TARMA (UPE-TARMA) models impose no mathematical structure on the time evolution of their parameters, which are thus free to change with time. Such a model is thus directly parameterized in terms of its TV parameters $a_i[t], c_i[t], \sigma_e^2[t]$, and a specific model structure, say $\mathcal{M}_{UPE}$, is defined by the representation orders n_a, n_c, that is

$$\mathcal{M}_{UPE}\triangleq\{n_\alpha, n_c\} \tag{6}$$

3.2. Stochastic parameter evolution TARMA models

Stochastic parameter evolution TARMA models impose stochastic structure on the time evolution of their parameters. The latter are thus assumed to be autocorrelated random variables allowed to change with time, but with their evolution being subject to certain smoothness constraints. These are often referred to as *smoothness priors constraints*, and the models are thus referred to as *smoothness priors TARMA* (SP-TARMA) models. The smoothness priors constraints typically are stochastic difference equations of the forms

$$\Delta^\kappa a_i[t]=w_{a_i}[t], \quad w_{a_i}[t]\sim\text{NID}(0,\sigma_{w_{a_i}}^2[t]) \tag{7a}$$

$$\Delta^\kappa c_i[t]=w_{c_i}[t], \quad w_{c_i}[t]\sim\text{NID}(0,\sigma_{w_{c_i}}^2[t]) \tag{7b}$$

acting on each one of the AR and MA parameters. In these expressions κ designates the difference equation order, Δ^κ the κ−th order difference operator ($\Delta^\kappa\triangleq(1-\mathcal{B})^\kappa$; where $\mathcal{B}$ the backshift operator $\mathcal{B}^i x[t]\triangleq x[t-i]$) and $w_{a_i}[t], w_{c_i}[t]$ zero-mean, uncorrelated (white) and mutually uncorrelated, and uncrosscorrelated with $e[t]$, Gaussian sequences with potentially TV variances. The degree of smoothness of the time evolution of each parameter is controlled by the corresponding white sequence variance, and increases for decreasing variance. A specific SP-TARMA model structure is defined by the model orders n_a, n_c and the smoothness constraints order κ (the latter being typically assumed to be common for all AR and

MA parameters):

$$\mathcal{M}_{SP} \triangleq \{n_a, n_c, \kappa\} \tag{8}$$

3.3. Deterministic parameter evolution TARMA models

Deterministic parameter evolution TARMA models impose deterministic structure on the time evolution of their parameters. This is achieved by postulating model parameters as deterministic functions of time belonging to specific *functional subspaces* [2,7,14,22, Ch. 6, 23,30]. These models are specifically referred to as *functional series TARMA* (FS-TARMA) models. Their AR and MA parameters, as well as their innovations variance, are thus expanded on the selected functional subspaces

$$\mathcal{F}_{AR} \triangleq \{G_{b_a(1)}[t], \ldots, G_{b_a(p_a)}[t]\}, \qquad \mathcal{F}_{MA} \triangleq \{G_{b_c(1)}[t], \ldots, G_{b_c(p_c)}[t]\}$$

$$\mathcal{F}_{\sigma_e^2} \triangleq \{G_{b_s(1)}[t], \ldots, G_{b_s(p_s)}[t]\}$$

Each functional subspace consists of a set of orthogonal *basis functions* selected from a suitable family (such as a polynomial family, a trigonometric family, and so on). The AR, MA, and variance subspace dimensionalities are indicated as p_a, p_c, p_s, respectively, while the indices $b_a(i)$ $(i = 1, \ldots, p_a)$, $b_c(i)$ $(i = 1, \ldots, p_c)$ and $b_s(i)$ $(i = 1, \ldots, p_s)$ designate the specific basis functions of a particular family that are included in each subspace. The TV AR and MA parameters and the innovations variance of an FS-TARMA$(n_a, n_c)_{[p_a, p_c, p_s]}$ model are then expressed as

$$a_i[t] \triangleq \sum_{j=1}^{p_a} a_{i,j} G_{b_a(j)}[t], \quad c_i[t] \triangleq \sum_{j=1}^{p_c} c_{i,j} G_{b_c(j)}[t], \quad \sigma_e^2[t] \triangleq \sum_{j=1}^{p_s} s_j G_{b_s(j)}[t]$$

with $a_{i,j}$, $c_{i,j}$, and s_j designating the AR, MA, and innovations variance, respectively, *coefficients of projection*. An FS-TARMA model is thus parameterized in terms of its projection coefficients $a_{i,j}, c_{i,j}, s_j$, while a specific model structure $\mathcal{M}_{FS}$ is defined by the model orders n_a, n_c, and the functional subspaces $\mathcal{F}_{AR}, \mathcal{F}_{MA}, \mathcal{F}_{\sigma_e^2}$.

$$\mathcal{M}_{FS} \triangleq \{n_a, n_c, \mathcal{F}_{AR}, \mathcal{F}_{MA}, \mathcal{F}_{\sigma_e^2}\} \tag{9}$$

FS-TARMA models achieve high parsimony, as they use a limited number of parameters. Through proper selection of the functional subspaces, FS-TARMA models may represent various types of evolution in the dynamics, including slow, fast or even discontinuous evolutions [7,8,13,17,22, p. 215, 31].

4. The identification problem and methods

Given a single, N-sample-long, nonstationary vibration response signal $x^N \triangleq \{x[1], \ldots, x[N]\}$ and a selected model class (unstructured, stochastic, or deterministic parameter evolution), the TARMA identification problem may be posed as the problem of selecting the corresponding model structure $\mathcal{M}$, the model AR/MA parameter vector $\boldsymbol{\theta}[t] \triangleq [a_1[t] \ldots a_{n_a}[t] \vdots c_1[t] \ldots c_{n_c}[t]]^{\mathrm{T}}$ and the innovations variance $\sigma_e^2[t]$ that best "fit" the observed response. *Model* "*fitness*" may be understood in various ways. In all of them a key role is assigned to the *model predictive ability*, that is the ability of a specific model in providing accurate one-step-ahead predictions.

Based on Eq. (5) it is straightforward to verify that the minimum mean square error one-step-ahead prediction $\hat{x}[t|t-1]$ of the signal value $x[t]$ made at time $t-1$ is equal to

$$\hat{x}[t|t-1] = -\sum_{i=1}^{n_a} a_i[t] x[t-i] + \sum_{i=1}^{n_c} c_i[t] e[t-i] \tag{10}$$

(note that the hat generally designates estimator/estimate of the indicated quantity). Comparing Eq. (10) with the TARMA model of Eq. (5) it is also straightforward to verify that the one-step-ahead prediction error $\hat{e}[t|t-1] \triangleq x[t] - \hat{x}[t|t-1]$ is equal to $e[t]$.

Common "fitness" functions include the residual sum of squares (RSS), the Gaussian negative log-likelihood function, and the Bayesian information criterion (BIC) defined as [21, pp. 200–202, 33, pp. 505–507]

$$\mathrm{RSS} = \sum_{t=1}^{N} e^2[t] \tag{11}$$

$$-\ln \mathcal{L}(x^N) = \frac{N}{2} \ln 2\pi + \frac{1}{2} \sum_{t=1}^{N} \left(\ln(\sigma_e^2[t]) + \frac{e^2[t]}{\sigma_e^2[t]} \right) \tag{12}$$

$$\mathrm{BIC} = -\ln \mathcal{L}(x^N) + \frac{\ln N}{2} d \tag{13}$$

respectively. In the BIC expression d designates the number of independently estimated model parameters. Also note that the BIC consists of the superposition of the negative log-likelihood function and a term that penalizes the model size (complexity), thus discouraging model overfitting. For this reason it may be used for both parameter estimation and model structure selection. Nevertheless, it may not be formally used within the context of UPE-TARMA and SP-TARMA models, the parameters of which are (recursively) updated at each time instant. In principle, a model is thus identified as that minimizing a selected "fitness" function.

For purposes of practicality and conceptual simplicity, the identification problem is commonly distinguished into two subproblems: (a) *model parameter estimation* and (b) *model structure selection*. Model parameter estimation is subsequently discussed first, as it is an essential part of model structure selection as well.

4.1. Model parameter estimation

Model parameter estimation refers to the determination, for a given model form and structure, of the AR/MA parameter vector $\boldsymbol{\theta}[t]$ and the residual variance $\sigma_e^2[t]$ at all time instants $t = 1, \ldots, N$.

4.1.1. Unstructured parameter evolution TARMA models

The estimation of UPE-TARMA models is often based on *recursive* methods, which update the parameter vector estimate each time a new signal sample becomes available [25,33, ch. 11, 34,35]. Presently, the *recursive maximum likelihood* (RML) algorithm [33, p. 372] is used for UPE-TARMA model parameter estimation and the corresponding method is thus referred to as RML-TARMA. A summary of the method is provided in Table 1. The quantity λ of these equations is referred to as the *forgetting factor*; its selection is critical and represents the basic tradeoff between tracking ability in the dynamics and achievable parameter accuracy.

Following parameter estimation, the innovations (one-step-ahead prediction error) variance $\sigma_e^2[t]$ may be estimated by using a window of length $2K+1$, centered at the time instant t, that slides over the prediction error (residual) sequence, that is

$$\hat{\sigma}_e^2[t] = \frac{1}{2K+1} \sum_{\tau=t-K}^{t+K} \hat{e}^2[\tau|\tau-1] \tag{14}$$

4.1.2. Stochastic parameter evolution TARMA models

Model parameter estimation for the SP-TARMA models of Eq. (7) may be developed by setting the latter, along with the TARMA model expression of Eq. (5), into linear state space form.

It can be shown that in the general (κ−th order) smoothness constraint SP-TARMA(n_a, n_c) model is expressed as [2,6]

$$\boldsymbol{z}[t] = \boldsymbol{F} \cdot \boldsymbol{z}[t-1] + \boldsymbol{G} \cdot \boldsymbol{w}[t], \quad x[t] = \boldsymbol{h}^{\mathrm{T}}[t, \boldsymbol{z}^{t-1}] \cdot \boldsymbol{z}[t] + e[t] \tag{15a}$$

$$\begin{bmatrix} \boldsymbol{w}[t] \\ \hline e[t] \end{bmatrix} \sim \mathrm{NID}\left(\begin{bmatrix} 0 \\ \vdots \\ 0 \end{bmatrix}, \left[\begin{array}{ccc|c} & \boldsymbol{Q}[t] & & \begin{matrix} 0 \\ \vdots \\ 0 \end{matrix} \\ \hline 0 & \ldots & 0 & \sigma_e^2[t] \end{array}\right] \right), \quad \boldsymbol{Q}[t] = \sigma_w^2[t] \cdot \boldsymbol{I}_{n_a+n_c} \tag{15b}$$

with:

$$\boldsymbol{h}[t, \boldsymbol{z}^{t-1}] \triangleq [-x[t-1] \ldots -x[t-n_a] \vdots e[t-1, \boldsymbol{z}^{t-1}] \ldots e[t-n_c, \boldsymbol{z}^{t-n_c}] \vdots 0 \ldots 0]^{\mathrm{T}}_{\kappa\cdot(n_a+n_c)\times 1} \tag{15c}$$

$$\boldsymbol{z}[t] \triangleq [a_1[t] \ldots a_{n_a}[t]\ c_1[t] \ldots c_{n_c}[t] \vdots \ldots \vdots a_1[t-\kappa+1] \ldots a_{n_a}[t-\kappa+1]\ \ c_1[t-\kappa+1] \ldots c_{n_c}[t-\kappa+1]]^{\mathrm{T}}_{\kappa\cdot(n_a+n_c)\times 1} \tag{15d}$$

$$\boldsymbol{w}[t] \triangleq [w_{a_1}[t]\ \ w_{a_2}[t] \ldots w_{a_{n_a}}[t] \vdots w_{c_1}[t]\ \ w_{c_2}[t] \ldots w_{c_{n_c}}[t]]^{\mathrm{T}}_{(n_a+n_c)\times 1} \tag{15e}$$

Table 1
RML-TARMA estimation.

Estimator update	$\hat{\boldsymbol{\theta}}[t] = \hat{\boldsymbol{\theta}}[t-1] + \boldsymbol{k}[t]\hat{e}[t\|t-1]$
Prediction error	$\hat{e}[t\|t-1] = x[t] - \hat{x}[t\|t-1] = x[t] - \boldsymbol{\phi}^{\mathrm{T}}[t]\hat{\boldsymbol{\theta}}[t-1]$
Gain	$\boldsymbol{k}[t] = \dfrac{\boldsymbol{P}[t-1]\boldsymbol{\psi}[t]}{\lambda + \boldsymbol{\psi}^{\mathrm{T}}[t]\boldsymbol{P}[t-1]\boldsymbol{\psi}[t]}$
"Covariance" update	$\boldsymbol{P}[t] = \dfrac{1}{\lambda}\left(\boldsymbol{P}[t-1] - \dfrac{\boldsymbol{P}[t-1]\boldsymbol{\psi}[t]\boldsymbol{\psi}^{\mathrm{T}}[t]\boldsymbol{P}[t-1]}{\lambda + \boldsymbol{\psi}^{\mathrm{T}}[t]\boldsymbol{P}[t-1]\boldsymbol{\psi}[t]}\right)$
Filtering	$\boldsymbol{\psi}[t] + \hat{c}_1[t-1]\boldsymbol{\psi}[t-1] + \cdots + \hat{c}_{n_c}[t-1]\boldsymbol{\psi}[t-n_c] = \boldsymbol{\phi}[t]$
A-posteriori error	$\hat{e}[t\|t] = x[t] - \boldsymbol{\phi}^{\mathrm{T}}[t]\hat{\boldsymbol{\theta}}[t]$
$\boldsymbol{\phi}[t] \triangleq [-x[t-1] \ldots -x[t-n_\alpha] \vdots \hat{e}[t-1\|t-1] \ldots\ \hat{e}[t-n_c\|t-n_c]]^{\mathrm{T}}$	

Initialization: $\hat{\boldsymbol{\theta}}[0] = \boldsymbol{0}$, $\boldsymbol{P}[0] = \alpha \boldsymbol{I}$ with α designating a "large" positive number. The signal and a-posteriori error initial values are set to zero.

$\boldsymbol{z}^t$ designating a vector containing all state vectors $\boldsymbol{z}[t]$ up to time t, and F, G matrices of the following forms (depending upon the value of κ):

$$\kappa=1: \quad \boldsymbol{F}\triangleq\boldsymbol{I}_{n_a+n_c}, \quad \boldsymbol{G}\triangleq\boldsymbol{I}_{n_a+n_c}$$

$$\kappa=2: \quad \boldsymbol{F}\triangleq\left[\begin{array}{c|c} 2\cdot\boldsymbol{I}_{n_a+n_c} & -\boldsymbol{I}_{n_a+n_c} \\ \hline \boldsymbol{I}_{n_a+n_c} & \boldsymbol{0}_{n_a+n_c}\end{array}\right], \quad \boldsymbol{G}\triangleq\left[\begin{array}{c}\boldsymbol{I}_{n_a+n_c}\\ \hline \boldsymbol{0}_{n_a+n_c}\end{array}\right]$$

$$\kappa=3: \quad \boldsymbol{F}\triangleq\left[\begin{array}{c|c|c} 3\cdot\boldsymbol{I}_{n_a+n_c} & -3\cdot\boldsymbol{I}_{n_a+n_c} & \boldsymbol{I}_{n_a+n_c} \\ \hline \boldsymbol{I}_{n_a+n_c} & \boldsymbol{0}_{n_a+n_c} & \boldsymbol{0}_{n_a+n_c} \\ \hline \boldsymbol{0}_{n_a+n_c} & \boldsymbol{I}_{n_a+n_c} & \boldsymbol{0}_{n_a+n_c}\end{array}\right], \quad \boldsymbol{G}\triangleq\left[\begin{array}{c}\boldsymbol{I}_{n_a+n_c}\\ \hline \boldsymbol{0}_{n_a+n_c}\\ \hline \boldsymbol{0}_{n_a+n_c}\end{array}\right]$$

and so on, where $\boldsymbol{I}_n$ and $\boldsymbol{0}_n$ designate the $n\times n$ dimensional identity and zero matrices, respectively. As indicated by the above expressions, $\boldsymbol{z}[t]$ forms a *state vector* [Eq. (15a)], whereas $\boldsymbol{w}[t]$ consists of the scalar innovations entering in each constraint expression.

The second of Eq. (15a) is a nonlinear function of $\boldsymbol{z}[t]$. SP-TARMA parameter estimation may be then based on an extended least squares (ELS)-like algorithm, by replacing the theoretical prediction errors $e[t,\boldsymbol{z}^t]$ in Eq. (15c) with their respective posterior estimates $\hat{e}[t|t]$ (which are then treated as measurements). SP-TARMA parameter estimation may be then achieved via the ordinary Kalman filter (KF) algorithm with:

$$\boldsymbol{h}[t]=[-x[t-1]\ldots-x[t-n_a]\vdots\hat{e}[t-1|t-1]\ldots\hat{e}[t-n_c|t-n_c]\vdots 0\ldots 0]^{\mathrm{T}}_{\kappa\cdot(n_a+n_c)\times 1}$$

$$\hat{e}[t|t]=x[t]-\boldsymbol{h}^{\mathrm{T}}[t]\cdot\hat{\boldsymbol{z}}[t|t] \tag{16}$$

A summary of a normalized version of the method, including a final backward smoothing phase, is provided in Table 2. It should be noted that the ratio $v[t]$ of the constraint model innovations variance $\sigma_w^2[t]$ (assumed to be common for all constraints) over the residual variance $\sigma_e^2[t]$, which is for simplicity assumed to be constant ($v[t]=v$) in the rest of the paper, constitutes a user selected design parameter that controls the equivalent memory of the estimation algorithm (similar to the forgetting factor in the RML-TARMA estimation method). Indeed, $v\to 0$ implies a locally deterministic (polynomial) parameter evolution, while $v\to\infty$ implies no structure on parameter evolution. Of course, it is also possible to optimize (estimate) v based on a suitable criterion (such as minimization of the RSS).

Innovations variance estimation may be achieved either via the scheme described in Ref. [29], or through that of the previous (RML-TARMA) method [Eq. (14)].

4.1.3. Deterministic parameter evolution TARMA models

Parameter estimation for FS-TARMA models consists of determining the AR/MA and innovations variance projection coefficient vectors

$$\boldsymbol{\vartheta}\triangleq[\boldsymbol{a}^{\mathrm{T}}\vdots\boldsymbol{c}^{\mathrm{T}}]^{\mathrm{T}}_{(n_ap_a+n_cp_c)\times 1} \quad \text{and} \quad \boldsymbol{s}\triangleq[s_1\ldots s_{p_s}]^{\mathrm{T}}_{p_s\times 1} \tag{17}$$

Table 2
Kalman filter and backward smoothing for the estimation of SP-TARMA models (normalized form).

Time update (***prediction***)	
State prediction	$\hat{\boldsymbol{z}}[t\|t-1]=\boldsymbol{F}\hat{\boldsymbol{z}}[t-1\|t-1]$
Prediction error	$\hat{e}[t\|t-1]=x[t]-\boldsymbol{h}^{\mathrm{T}}[t]\hat{\boldsymbol{z}}[t\|t-1]$
"Covariance" update	$\tilde{\boldsymbol{P}}[t\|t-1]=\boldsymbol{F}\tilde{\boldsymbol{P}}[t-1\|t-1]\boldsymbol{F}^{\mathrm{T}}+\boldsymbol{G}\tilde{\boldsymbol{Q}}[t]\boldsymbol{G}^{\mathrm{T}}$
Observation update (***filtering***)	
Gain	$\boldsymbol{k}[t]=\tilde{\boldsymbol{P}}[t\|t-1]\boldsymbol{h}[t](\boldsymbol{h}^{\mathrm{T}}[t]\tilde{\boldsymbol{P}}[t\|t-1]\boldsymbol{h}[t]+1)^{-1}$
State update	$\hat{\boldsymbol{z}}[t\|t]=\hat{\boldsymbol{z}}[t\|t-1]+\boldsymbol{k}[t]\hat{e}[t\|t-1]$
"Covariance" update	$\tilde{\boldsymbol{P}}[t\|t]=(\boldsymbol{I}-\boldsymbol{k}[t]\boldsymbol{h}^{\mathrm{T}}[t])\tilde{\boldsymbol{P}}[t\|t-1]$
Smoothing	
	$\boldsymbol{A}[t]=\tilde{\boldsymbol{P}}[t\|t]\boldsymbol{F}^{\mathrm{T}}\tilde{\boldsymbol{P}}^{-1}[t+1\|t]$
	$\hat{\boldsymbol{z}}[t\|N]=\hat{\boldsymbol{z}}[t\|t]+\boldsymbol{A}[t](\hat{\boldsymbol{z}}[t+1\|N]-\hat{\boldsymbol{z}}[t+1\|t])$
	$\tilde{\boldsymbol{P}}[t\|N]=\tilde{\boldsymbol{P}}[t\|t]+\boldsymbol{A}[t](\tilde{\boldsymbol{P}}[t+1\|N]-\tilde{\boldsymbol{P}}[t+1\|t])\boldsymbol{A}^{\mathrm{T}}[t]$
	$\tilde{\boldsymbol{P}}[t\|t]\triangleq\dfrac{\boldsymbol{P}[t\|t]}{\sigma_e^2[t]}, \quad \tilde{\boldsymbol{P}}[t\|t-1]\triangleq\dfrac{\boldsymbol{P}[t\|t-1]}{\sigma_e^2[t]}, \quad \tilde{\boldsymbol{Q}}[t]\triangleq\dfrac{\boldsymbol{Q}[t]}{\sigma_e^2[t]}=\underbrace{\dfrac{\sigma_w^2[t]}{\sigma_e^2[t]}}_{v[t]}\boldsymbol{I}_{n_a+n_c}$

Initialization: $\hat{\boldsymbol{z}}[0|0]=\boldsymbol{0}$, $\tilde{\boldsymbol{P}}[0|0]=\alpha\boldsymbol{I}$ with α designating a "large" positive number.

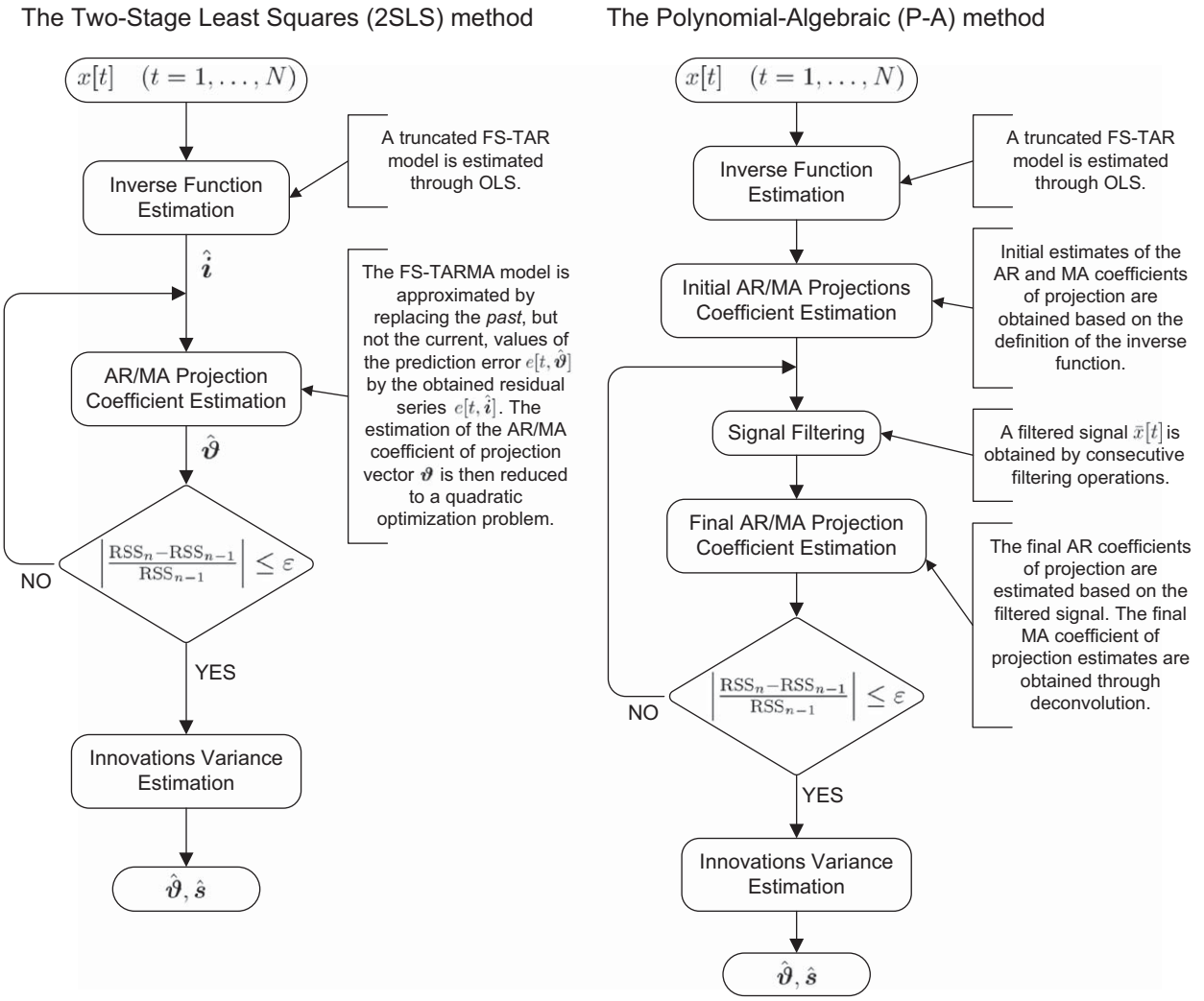

Fig. 1. Two multistage methods for FS-TARMA model identification.

respectively, with

$$\boldsymbol{a} \triangleq [a_{1,1} \ldots a_{1,p_a} \vdots \ldots \vdots a_{n_a,1} \ldots a_{n_a,p_a}]^{\mathrm{T}}_{(n_a p_a)\times 1}, \quad \boldsymbol{c} \triangleq [c_{1,1} \ldots c_{1,p_c} \vdots \ldots \vdots c_{n_c,1} \ldots c_{n_c,p_c}]^{\mathrm{T}}_{(n_c p_c)\times 1}$$

Estimation of the parameter vector $\boldsymbol{\vartheta}$ may be based on a *prediction error* criterion consisting of the sum of squares of the model's one-step-ahead prediction errors (RSS):

$$\hat{\boldsymbol{\vartheta}} = \underset{\boldsymbol{\vartheta}}{\operatorname{argmin}} \sum_{t=1}^{N} e^2[t, \boldsymbol{\vartheta}] \tag{18}$$

It is obvious, that the residual $e[t, \boldsymbol{\vartheta}]$ depends nonlinearly on the MA projection coefficient vector $\boldsymbol{c}$, implying that minimization of a prediction error criterion constitutes a nonquadratic problem that has to be tackled through nonlinear optimization techniques. This necessitates the use of rather accurate initial parameter values, which may be obtained through linear multistage methods (recursive methods may be also used).

Linear multistage methods attempt to approximate the original prediction error problem by a sequence of subproblems that may be tackled by means of linear techniques. Two such methods, the *two stage least squares* (2SLS) method [2,36] and the *polynomial-algebraic* (P-A) method [30] are outlined in Fig. 1.

Finally, the estimation of the innovations variance projection coefficients may be achieved by the following procedure. An initial, nonparametric, estimate of the innovations variance may be based on a sliding time window that uses the estimated residual series $e[t, \hat{\boldsymbol{\vartheta}}]$ [as in Eq. (14)], and an estimate of the projection coefficient vector $\boldsymbol{s}$ may be subsequently obtained by fitting the estimated variance $\hat{\sigma}^2_e[t]$ to a selected functional subspace $\mathcal{F}_{\sigma^2_e}$. This leads to the overdetermined set

of equations

$$\hat{\sigma}_e^2[t] = \sum_{j=1}^{p_s} s_j G_{b_s(j)}[t] = \boldsymbol{g}^{\mathrm{T}}[t]\boldsymbol{s} \tag{19}$$

with $\boldsymbol{g}[t] \triangleq [G_{b_s(1)}[t]\ G_{b_s(2)}[t] \ldots G_{b_s(p_s)}[t]]^{\mathrm{T}}_{p_s \times 1}$, which is then solved in a least squares sense.

4.2. Model structure selection

Model structure selection refers to the estimation of the proper model structure within a selected model class. The model structure includes the AR and MA orders n_a and n_c, respectively, as well as additional structural parameters that depend on the particular model class considered [see Eqs. (6), (8), and (9) that define the model structure $\mathcal{M}_{UPE}/\mathcal{M}_{SP}/\mathcal{M}_{FS}$ for each class].

A search scheme for locating the best "fitness" model, is subsequently discussed for the most general case of FS-TARMA models which have the "richest" structure and are characterized by the maximum number of "structural" parameters. The key characteristic of this scheme is the approximate decomposition of the "structure" selection problem into two subproblems: (i) model order (n_a, n_c) selection and (ii) functional subspace $[p_a, p_c, p_s, b_a(j), b_c(j), b_s(j)]$ selection.

Phase I: model order selection: In order to "decouple" the selection of the model orders from that of functional subspaces, their interaction has to be minimized. This may be achieved by ensuring functional subspace adequacy by initially adopting an "extended" (high dimensionality) and "complete" (in the sense of including all consecutive functions up to the subspace dimensionality) functional subspaces. Using them, model order selection may be achieved through trial and error techniques based on the optimization of the fitness function.

Phase II: functional subspace selection: The aim of this phase is the optimization of the functional subspaces, in the sense of increasing the representation parsimony without significantly reducing model accuracy. This may be accomplished through trial and error techniques detecting "excess" basis functions by using either the fitness function or the aggregate parameter deviation (APD). The latter constitutes a measure for the aggregate deviation of the parameter trajectories of the current model from those of the initial (phase I) model

$$\mathrm{APD} \triangleq \sum_{i=1}^{n_a} \Delta a_i + \sum_{i=1}^{n_c} \Delta c_i + \Delta s \tag{20}$$

with

$$\Delta q_i \triangleq \frac{\sum_{t=1}^{N} |q_i^{\circ}[t] - q_i[t]|}{\sum_{t=1}^{N} |q_i^{\circ}[t]|}$$

in which $q_i^{\circ}[t]$ designates the initial model AR/MA/innovations variance parameter trajectories and $q_i[t]$ the respective trajectories of the currently considered model. Basis functions may be thus successively dropped (one at a time) as long as no significant changes in the fitness function or in the APD are produced.

A specific basis function family (such as a proper polynomial or trigonometric family) is generally pre-selected (although not the specific functions that define the model's functional subspaces). This pre-selection may be based on various factors, including physical insight, prior knowledge, or experience. Yet, it should be stressed that, although the pre-selection does affect the final identified model structure (thus the model "size") and parameters, it does *not* critically affect model accuracy (also see [37] in this context). The reason is that essentially any functional family may be used for approximating any given curve with arbitrary accuracy as long as a sufficient number of functions is used [38, p. 77]. In practice a good strategy is to use two or more families, obtain the best (according to the selected "fitness" function) under each one, have them properly validated, and finally select the globally optimum (best) model.

A few words are finally in order regarding model validation: any identified model should be normally validated. Although such validation may be based on various criteria, which may generally depend on the model's intended use, the Gaussianity and, in particular, the whiteness of the identified model's one-step-ahead prediction error (residual) sequence are parts of standard validation procedures. Due to the TV nature of the model residual variance, the usual residual whiteness tests are not applicable in the present case. Yet, a simple test that may be applied is the residual sign test—see Refs. [2,39, pp. 192–198].

5. The laboratory time-varying structure and preliminary analysis

The laboratory TV structure is shown in Fig. 2. It is a bridge with heavy vehicle type structure consisting of a steel beam of dimensions $2670 \times 50 \times 12\,\mathrm{mm}$ $(L \times W \times H)$, clamped close to its both ends on vertical stands, and a steel cylindrical mass of dimension $52.5 \times 75.0\,\mathrm{mm}$ $(R \times H)$ sliding on it (being pulled by a DC motor with constant speed u). As the ratio of the two masses is significant $(m/M \approx 0.4)$, the structure is clearly TV, with the rate of variation depending on the selected speed u. Evidently, the structure belongs to the subclass of continuously variable configuration structures, and the configuration vector may be defined as pointing at the moving mass position. This structure has been used in a previous study by employing FS-TARMA models [11].

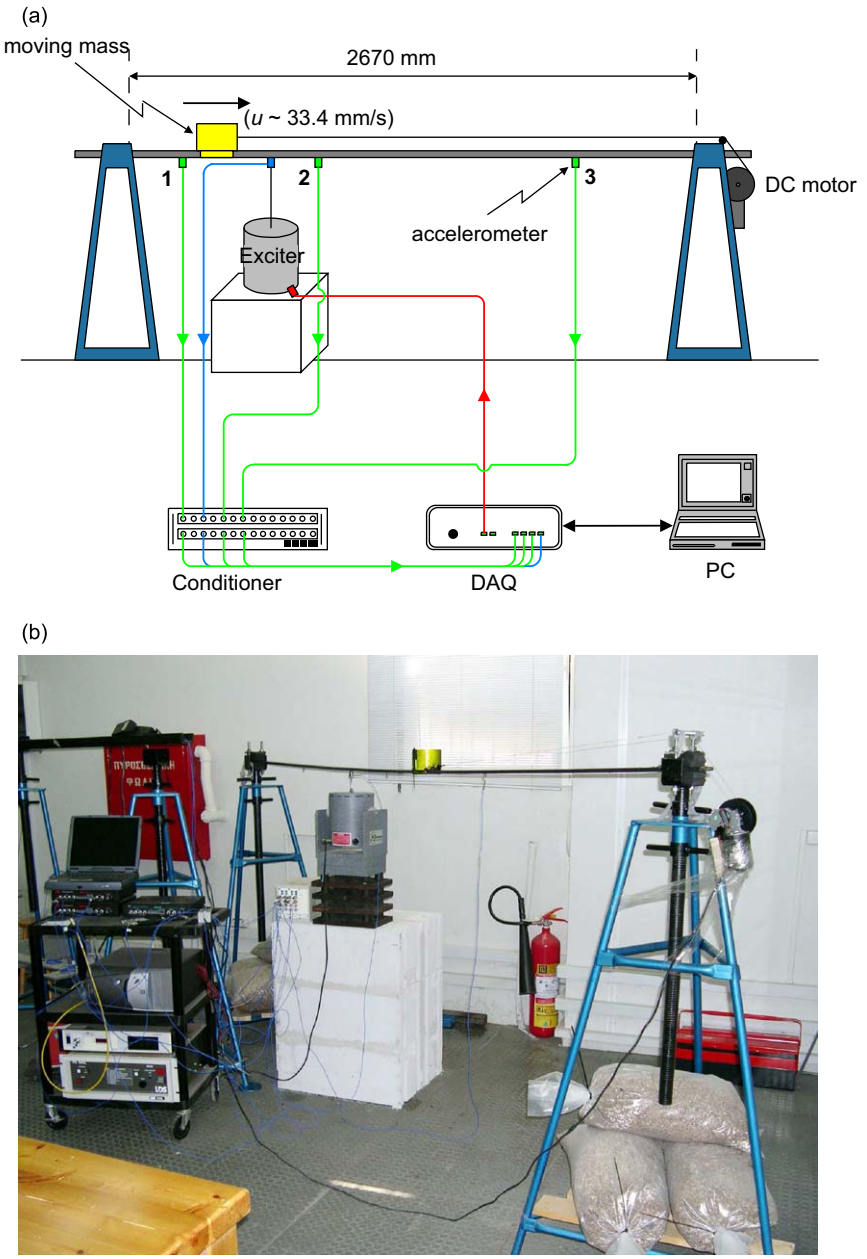

Fig. 2. The laboratory TV structure. A bridge with heavy vehicle type structure consisting of a steel beam, clamped close to its both ends on vertical stands, and a cylindrical mass sliding on it at a selected speed: (a) schematic diagram and (b) photo of the experimental setup [11].

The beam is subject to zero-mean, Gaussian, random force excitation vertically exerted through an electromechanical shaker (MB Dynamics Modal Exciter 50A, max load 225 N) equipped with a stinger. The resulting beam vibration is measured at three selected locations [Fig. 2(a); locations 1–3] by piezoelectric accelerometers (PCB 352A10 ICP accelerometers, frequency range 0.003–10 kHz, sensitivity $\sim$1.052 mV/m/s^2), although only that at location 3 is presently used. The measured vibration signals are conditioned and subsequently driven into a 20–42 SigLab data acquisition module (featuring four 20-bit simultaneously sampled A/D, two 16-bit D/A channels, and analog anti-aliasing filters).

In a single experiment the cylindrical mass traverses the beam (from left to right) once, at a constant speed of $u = 33.4$ mm/s. At this speed the structure may be characterized as relatively *slowly* TV. The vertical vibration (acceleration) signal is sampled at $f_s = 128$ Hz and is $N = 10,113$ samples (79.0078 s) long. The study focuses on the 4–60 Hz frequency range, hence the signal is digitally bandpass filtered.

The obtained response signal is shown in Fig. 3(a) and is evidently variance nonstationary. Nonparametric time–frequency analysis based on the short-time Fourier transform (STFT; 512-sample-long moving Hamming data

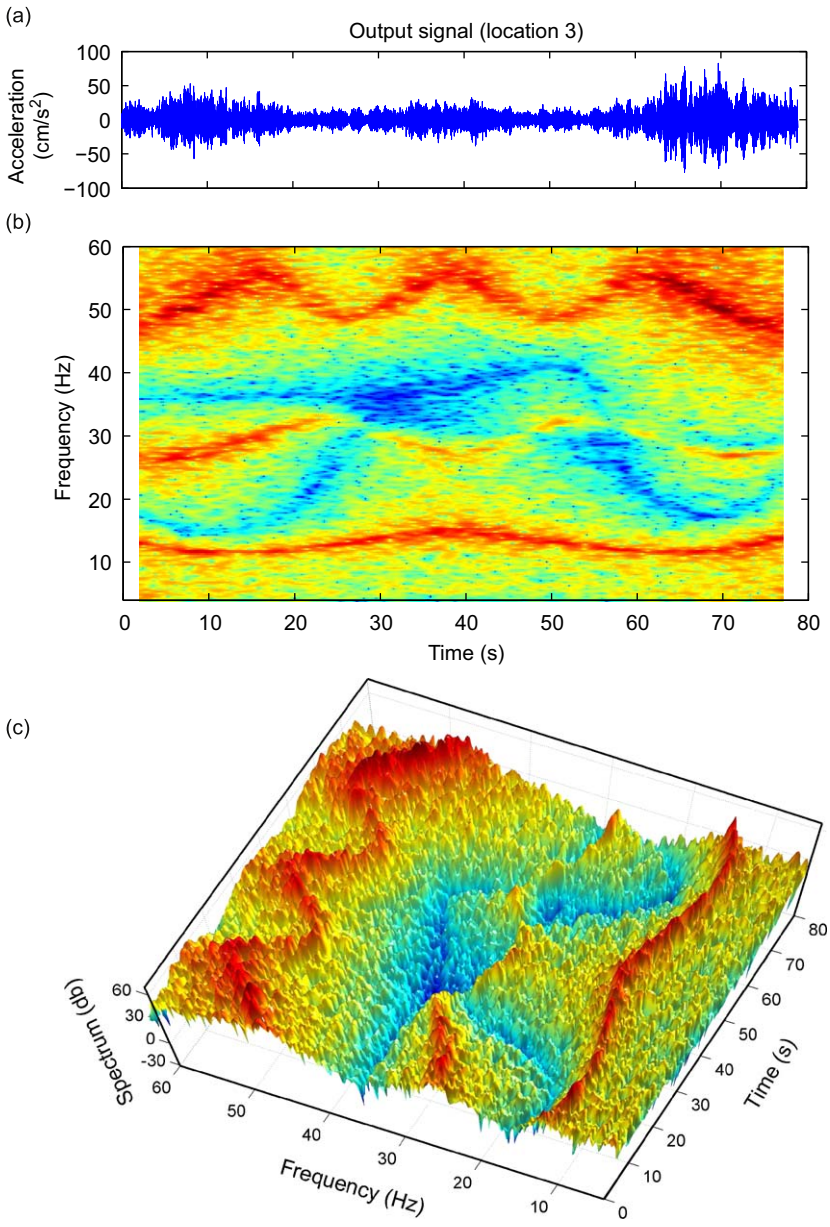

Fig. 3. The nonstationary vibration response and preliminary analysis: (a) the vibration response signal (sampling frequency $f_s = 128$ Hz, signal length $N = 10,113$ samples or 79.0078 s), (b) 2D plot of the non-parametrically obtained TV PSD estimate (STFT employing a 512-sample-long moving Hamming data window advanced by one sample each time), and (c) 3D plot of the non-parametrically obtained TV PSD estimate.

window advanced by one sample each time) yields the TV power spectral density (PSD) function of Figs. 3(b) and (c). Evidently, the structure is characterized by three TV vibration modes (three natural frequencies) and the response signal is nonstationary in terms of its spectral content as well.

6. Output-only identification results

Model order estimation, which is the part of model structure selection shared by all parametric methods, is based on the successive identification of TARMA(n,n) models of orders $n = 2,\ldots,12$ and the optimization of a proper "fitness" function—specifically the RSS in the RML-TARMA and SP-TARMA cases, and the BIC in the FS-TARMA case.

In the RML-TARMA case the RSS leads to a UPE-TARMA(8,8) model estimated with forgetting factor $\lambda = 0.9905$ and initial covariance matrix $10^4\boldsymbol{I}$. Note that this result is optimized with respect to the forgetting factor (an exhaustive search

has been implemented). Furthermore, in order to reduce the effects of arbitrary initial conditions in the estimation, three sequential passes (forward, backward, and final forward) are executed over the entire data record.

In the SP-TARMA case and for each estimated model, three possible orders are considered for the smoothness priors constraints, namely $\kappa = 1, 2, 3$, while optimization (of the RSS) with respect to ratio of the smoothness priors constraints innovations variance over the residual variance v is also carried out. Like in the RML-TARMA case, three sequential passes (forward, backward, and a final forward) are executed over the entire data record, while a final backward smoothing algorithm is also applied. For the initialization of the KF algorithm the covariance matrix is set to $10^4\boldsymbol{I}$. The $\kappa = 1, 2$ selections provide reasonable results, with almost identical RSS values for large model orders ($n_a, n_c > 7$; see Fig. 4). Yet, the $\kappa = 1$ selection leads to somewhat increased variability in the TV natural frequency and PSD estimates. The $\kappa = 3$ selection leads to numerical problems as the obtained v is very small (10^{-16}). Based on the above, the selected model is SP-TARMA(8,8) with $\kappa = 2$ and $\hat{v} = 2.757 \times 10^{-11}$.

In the FS-TARMA case functional bases spanned by trigonometric functions of the form

$$G_0[t] = 1, \quad G_{2k-1}[t] = \sin\left(\frac{k\pi(t-1)}{N-1}\right), \quad G_{2k}[t] = \cos\left(\frac{k\pi(t-1)}{N-1}\right)$$

with $t = 1, \ldots, N$ and $k = 1, 2, \ldots$ are employed. Their selection is motivated by the nonparametric estimates of Figs. 3(b) and (c). Model order selection is achieved using phase I of the search scheme described in Section 4.2, the BIC, and an extended and complete functional subspace of dimensionality 21 ($p_a = p_c = p_s = 21$). An FS-TARMA $(8,8)_{[21,21,21]}$ model is thus initially selected as adequate [see Fig. 5(a)]. Functional subspace selection is subsequently pursued based on phase II

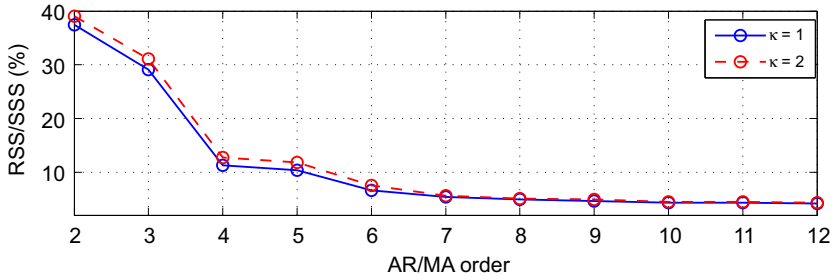

Fig. 4. SP-TARMA model structure selection. AR/MA order and smoothness constraints order selection based on the RSS/SSS function.

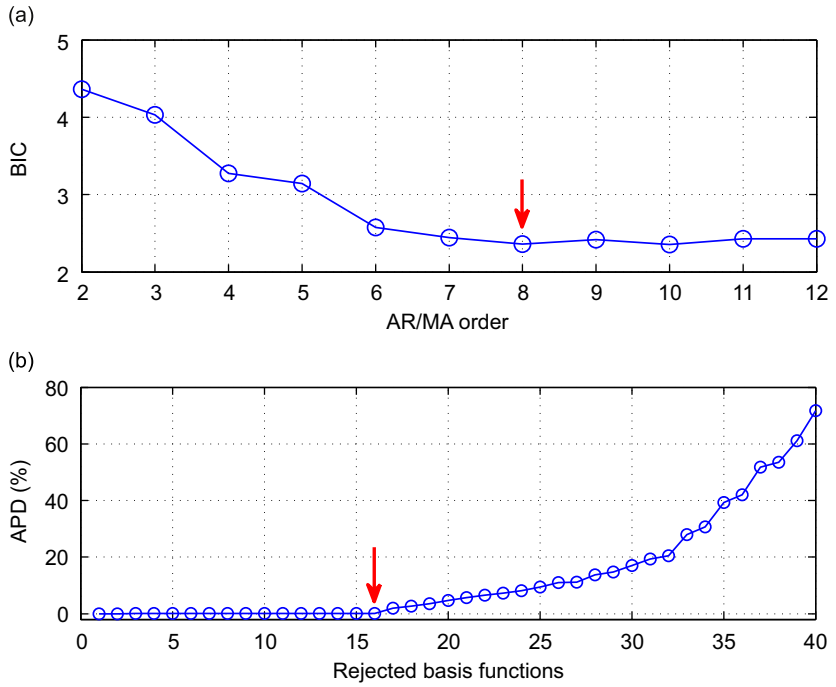

Fig. 5. FS-TARMA model structure selection: (a) AR/MA order selection based on the BIC using an extended and complete functional subspace ($p_a = p_c = p_s = 21$) and (b) combined AR/MA functional subspace selection. APD values obtained by iteratively rejecting the least significant basis function versus the number of rejected functions. The model just before the first significant increment is selected (16 functions are presently rejected and 26 are maintained in the AR/MA subspaces).

and the APD criterion combined with the backward procedure. This leads to the AR/MA functional subspaces [Fig. 5(b)]

$$\mathcal{F}_{AR} = \{G_0[t], \ldots, G_{10}[t]\}, \quad \mathcal{F}_{MA} = \{G_0[t], \ldots, G_{14}[t]\}$$

and, similarly, to the innovations variance subspace

$$\mathcal{F}_{\sigma_e^2} = \{G_0[t], \ldots, G_6[t], G_8[t], G_9[t], G_{10}[t], G_{12}[t], G_{13}[t], G_{14}[t], G_{17}[t], G_{19}[t]\}.$$

Hence an FS-TARMA $(8,8)_{[11,15,15]}$ model is finally selected (further details in [11]).

The three identified TARMA models are validated, whereas their characteristics are summarized in Table 3.

The obtained RSS normalized by the series sum of squares (RSS/SSS) and the negative log-likelihood function of the estimated TARMA models are depicted in Fig. 6(a). Indicative one-step-ahead signal predictions obtained by the estimated

Table 3
Identification methods, their characteristics, and the identified models.

Model class	Identification method	Method characteristics	Identified model
Unstructured parameter evolution	RML-TARMA	$\lambda = 0.9905$ $\alpha = 10^4$	UPE-TARMA(8,8)
Stochastic parameter evolution	SP-TARMA	$v = 2.757 \times 10^{-11}$ $\alpha = 10^4$	SP-TARMA$(8,8)_{\kappa=2}$
Deterministic parameter evolution	FS-TARMA	Prediction error method Gauss–Newton optimization	FS-TARMA$(8,8)_{[11,15,15]}$

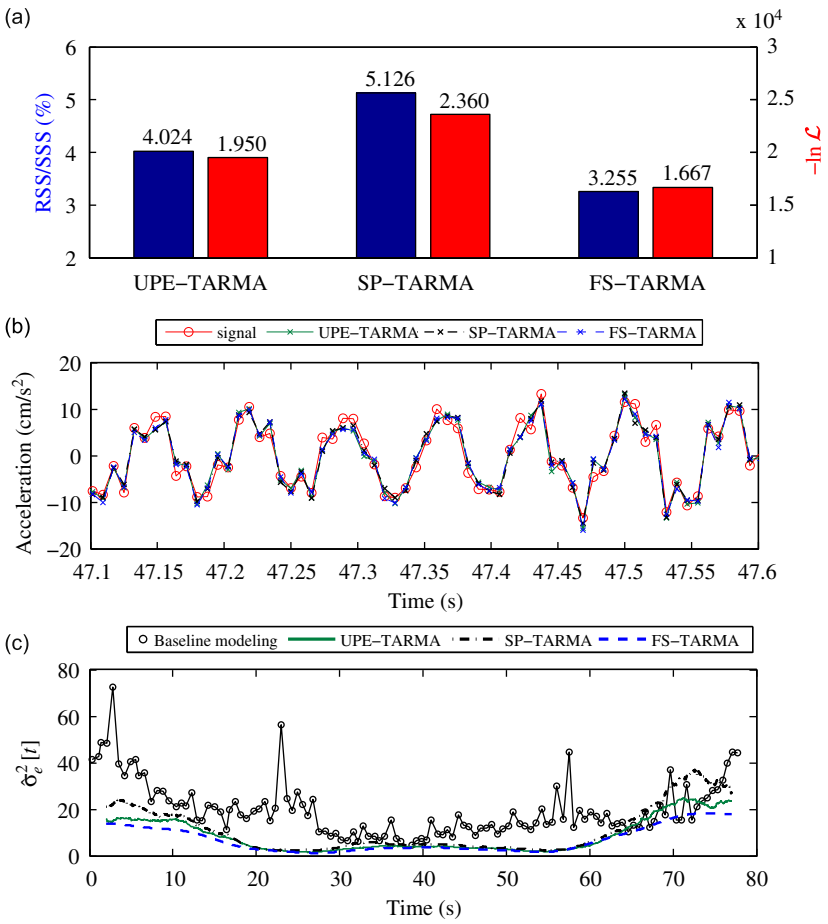

Fig. 6. Comparative TARMA identification results: (a) the RSS/SSS and the negative log-likelihood function for the estimated TARMA models, (b) segment of the vibration response signal and TARMA-based one-step-ahead predictions, and (c) the residual variance for the estimated TARMA models (although not directly comparable, the "frozen-configuration" innovations variance is also provided).

TARMA models are (for a short time segment of the signal) compared to the actual signal values in Fig. 6(b). It is observed that all methods provide more or less good predictions, with the FS-TARMA model achieving the best prediction accuracy (RSS/SSS = 3.255%), followed by the RML-estimated UPE-TARMA model, and, finally, the SP-TARMA model. It should be mentioned that the RSS/SSS and negative log-likelihood function for the SP-TARMA(8,8) model may be reduced somewhat (to 4.893 and 2.336×10^4, respectively) when using first order ($\kappa = 1$) smoothness priors constraints. As already mentioned, this model is nevertheless not selected, as the corresponding natural frequency estimates and the TV PSD exhibit higher variability.

The residual variance estimates for the three TARMA models are compared in Fig. 6(c), in which the baseline model innovations variance (although not directly comparable; description in the next paragraph) is presented as well. As it may observed, the FS-TARMA model provides, almost uniformly, the lowest variance, followed by the UPE-TARMA, and finally the SP-TARMA model.

Frozen-configuration baseline identification: In order to establish an additional basis for judging identification accuracy, a space-discretized version of the structure's frozen-configuration representation is obtained by "freezing" the mass at $M = 120$ equispaced locations and performing an equal number of *stationary* experiments. The stationary vibration response at location 3 on the beam is, in each case, obtained ($f_s = 128$ Hz, signal length $N = 3962$ samples) and a conventional (stationary) ARMA model is identified by using the linear multi stage (LMS) estimation method [40] and maximum-likelihood (ML) refinement [33, pp. 216–217]. This leads to $M = 120$ ARMA(8,8) models which constitute what is henceforth referred to as the *baseline* (frozen-configuration) representation of the structure.

7. Model-based dynamic analysis results

The TV structural dynamics are now recovered based on the identified models. The vibration response signal's frozen-time PSD is obtained as

$$S(\omega, t) = \left| \frac{1 + \sum_{i=1}^{n_c} c_i[t] \mathrm{e}^{-\mathrm{j}\omega T_s i}}{1 + \sum_{i=1}^{n_a} a_i[t] \mathrm{e}^{-\mathrm{j}\omega T_s i}} \right|^2 \sigma_e^2[t] \tag{21}$$

with the model parameters and innovations variance being replaced by their respective estimates, ω designating frequency in rad/s, T_s the sampling period in s, and j the imaginary unit. The system's frozen-time natural frequencies and damping ratios are computed as

$$\omega_{ni}[t] = \frac{|\ln \lambda_i[t]|}{T_s} \,(\mathrm{rad/s}) \quad \text{and} \quad \zeta_i[t] = -\cos(\arg(\ln \lambda_i[t])) \tag{22}$$

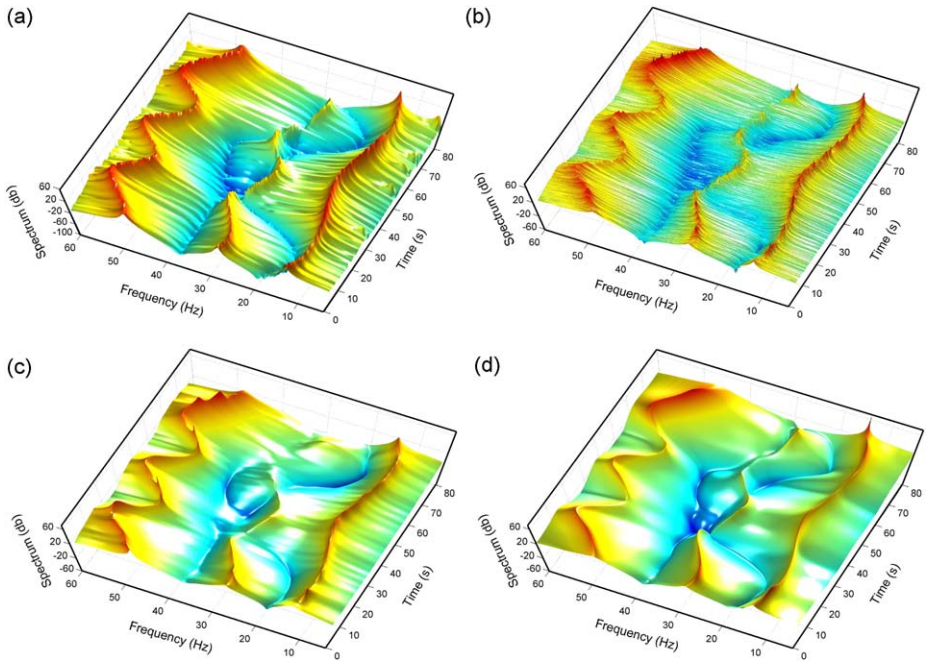

Fig. 7. Comparison of TV PSD estimates: (a) the "frozen-configuration" baseline estimate, (b) the UPE-TARMA(8,8) estimate, (c) the SP-TARMA$(8,8)_{\kappa=2}$ estimate, and (d) the FS-TARMA$(8,8)_{\{11,15,15\}}$ estimate.

respectively, with $\lambda_i[t]$ designating the i-th TV frozen model pole. The antiresonance natural frequencies and damping ratios are similarly obtained from the frozen model zeros.

The frozen-time PSD estimates corresponding to the three estimated TARMA(8,8) models are contrasted to that obtained from the frozen-configuration baseline modelling in Fig. 7. Obviously, all TARMA PSD estimates are in good overall agreement with their baseline counterpart. Yet, smoother, and also clear and informative, estimates are obtained based on the FS-TARMA and SP-TARMA models. On the other hand, the estimate obtained based on the UPE-TARMA model exhibits significantly more scatter.

Fig. 8 depicts the structure's TV natural frequency estimates along with their baseline model counterparts. Note that nonparametric PSD estimates (Welch-based; 512-sample-long Hamming data window) obtained during baseline identification by using the 120 measured signals are also shown in the background.

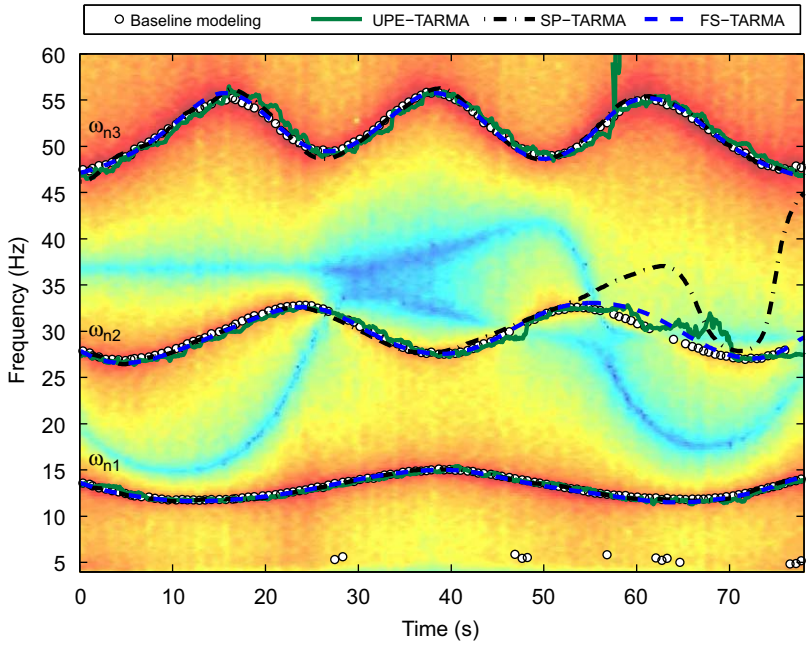

Fig. 8. Comparison of TV natural frequency estimates. The UPE-TARMA, SP-TARMA, and FS-TARMA based estimates are plotted against the "frozen-configuration" baseline estimates (baseline Welch-based PSD estimates are shown in the background).

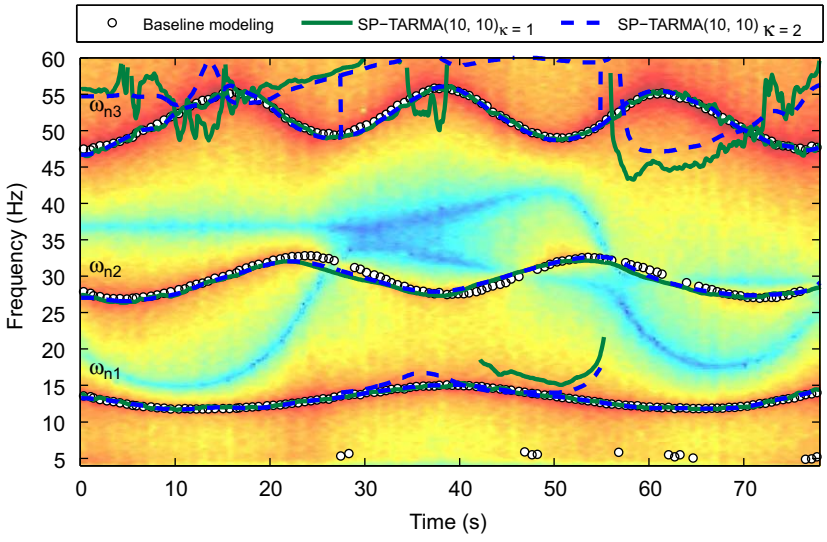

Fig. 9. Comparison of the SP-TARMA(10,10) based natural frequency estimates against the "frozen-configuration" baseline estimates (baseline Welch-based PSD estimates are shown in the background).

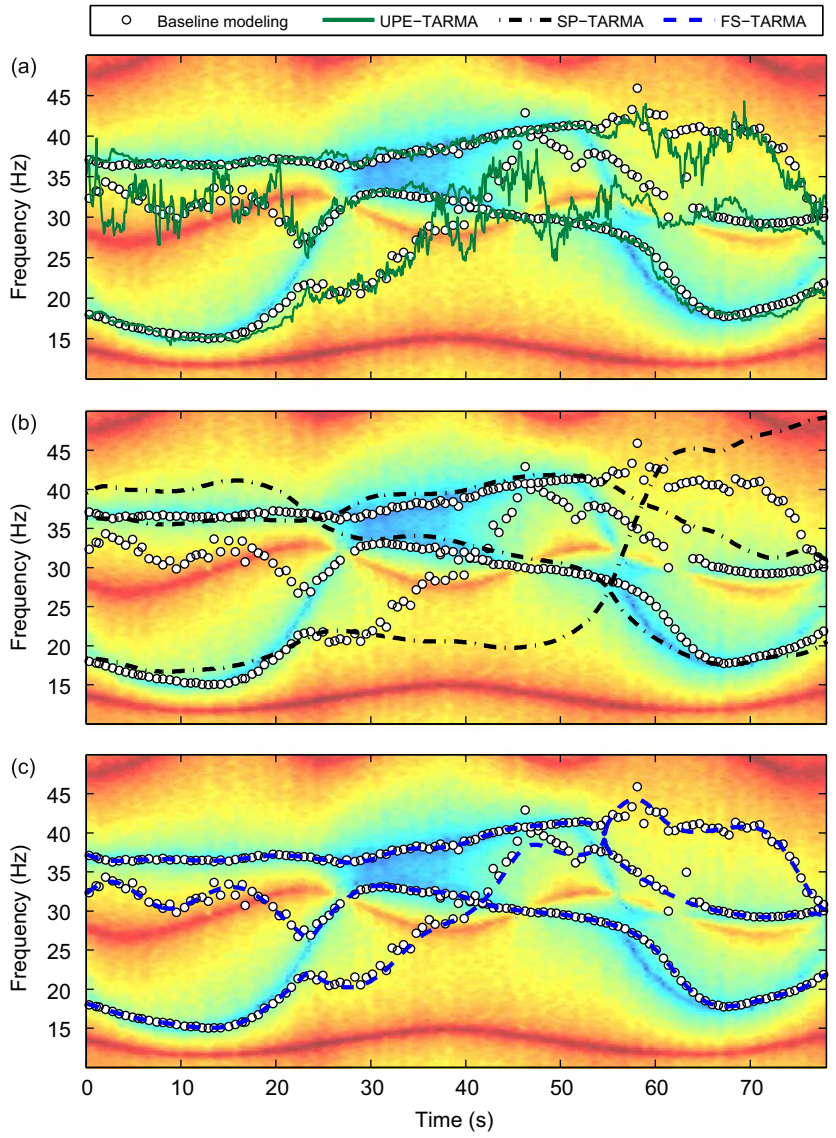

Fig. 10. Comparison of TV antiresonance natural frequency estimates. (a) The UPE-TARMA, (b) SP-TARMA, and (c) FS-TARMA based estimates plotted against the "frozen-configuration" baseline estimates (baseline Welch-based PSD estimates are shown in the background).

The UPE-TARMA estimates track their baseline counterparts adequately well, although with some scatter observed for the second and third natural frequency trajectories. On the other hand, the SP-TARMA estimates appear unable of tracking the second natural frequency during the last 30 s. This is probably due to pole-zero cancellations occurring. A possible remedy could be the increase of the model order to 10 or higher. Such an action, though, introduces false (computational) modes in the time–frequency plane (see Fig. 9) which are characterized by damping ratios smaller than 10 percent and being difficult to distinguish from the true modes. Finally, the excellent tracking of the natural frequencies achieved by the FS-TARMA estimates is certainly worth noting.

Similar comments may be made for the estimated frozen-time antiresonance natural frequencies (Fig. 10). The SP-TARMA based estimates seem unable of tracking the evolution of their baseline counterparts for significant periods of time, in contrast to the UPE-TARMA based estimates which exhibit a good overall agreement with them, but also significant scatter. On the other hand, the FS-TARMA based estimates clearly exhibit the best performance (Welch-based nonparametric PSD estimates obtained during baseline identification are also shown in the background).

8. Conclusions

An overview and comparative assessment of parametric TARMA methods for the identification and model-based analysis of TV structures under unobservable excitation was presented. The methods were classified according to the

mathematical structure imposed on the TV parameter evolution as unstructured parameter evolution, stochastic parameter evolution, and deterministic parameter evolution. A representative identification method (RML-TARMA, SP-TARMA, FS-TARMA) from each class was outlined.

The performance characteristics of the three classes of methods were examined through their application to the problem of identification and model-based dynamic analysis of a laboratory TV (continuously variable configuration) structure consisting of a beam with a mass moving on it. The frozen-configuration (baseline) characteristics of the structure were also extracted and used as an additional basis of comparison.

The three methods were compared to each other in terms of achievable prediction accuracy and model-based analysis. Although the TV structure used is characterized by relatively slowly varying dynamics, the best performance characteristics were achieved by the FS-TARMA method, followed by the RML-TARMA and, finally, the SP-TARMA method. This is also true for the model-based dynamics, including the resonance and antiresonance natural frequencies and the TV PSD of the vibration response, that were most accurately captured by the FS-TARMA method. These results came as no surprise, and, reveal good identification performance, owing to the deterministic nature of the time variation in the structural dynamics which is best reflected in the FS-TARMA models. Overall, the results demonstrate the parametric methods' applicability, effectiveness, and high potential for parsimonious and accurate identification and dynamic analysis of TV structures under unobservable excitation.

References

[1] J.S. Bendat, A.G. Piersol, *Random Data: Analysis and Measurements Procedures*, third ed., Prentice-Hall, Englewood Cliffs, NJ, 2000.
[2] A.G. Poulimenos, S.D. Fassois, Parametric time-domain methods for non-stationary random vibration modelling and analysis—a critical survey and comparison, *Mechanical Systems and Signal Processing* 20 (4) (2006) 763–816.
[3] A. Preumont, *Random Vibration and Spectral Analysis*, Kluwer Academic Publishers, Dordrecht, 1994.
[4] M.B. Priestley, *Non-Linear and Non-Stationary Time Series Analysis*, Academic Press, New York, 1988.
[5] J.K. Hammond, P.R. White, The analysis of non-stationary signals using time–frequency methods, *Journal of Sound and Vibration* 190 (3) (1996) 419–447.
[6] G. Kitagawa, W. Gersh, *Smoothness Priors Analysis of Time Series*, Springer, New York, 1996.
[7] S. Conforto, T. D'Alessio, Spectral analysis for non-stationary signals from mechanical measurements, *Mechanical Systems and Signal Processing* 13 (3) (1999) 395–441.
[8] K.A. Petsounis, S.D. Fassois, Non-stationary functional series TARMA vibration modelling and analysis in a planar manipulator, *Journal of Sound and Vibration* 231 (5) (2000) 1355–1376.
[9] R. Ghanem, F. Romeo, A wavelet-based approach for the identification of linear time-varying dynamical systems, *Journal of Sound and Vibration* 234 (4) (2000) 555–576.
[10] K. Liu, L. Deng, Identification of pseudo-natural frequencies of an axially moving cantilever beam using a subspace-based algorithm, *Mechanical Systems and Signal Processing* 20 (2006) 94–113.
[11] A.G. Poulimenos, S.D. Fassois, Output-only stochastic identification of a time-varying structure via functional series TARMA models, *Mechanical Systems and Signal Processing* 23 (4) (2009) 1180–1204.
[12] G. Dimitriadis, S.D. Fassois, A.G. Poulimenos, D. Shi, Identification and model updating of a non-stationary vibrating system, in: Proceedings of ASME Conference on Engineering Systems Design and Analysis, Manchester, UK, 2004.
[13] G.N. Fouskitakis, S.D. Fassois, Functional series TARMA modelling and simulation of earthquake ground motion, *Earthquake Engineering and Structural Dynamics* 31 (2) (2002) 399–420.
[14] O. Bardou, M. Sidahmed, Early detection of leakages in the exhaust and discharge systems of reciprocating machines by vibration analysis, *Mechanical Systems and Signal Processing* 8 (5) (1994) 551–570.
[15] A.G. Poulimenos, S.D. Fassois, Vibration-based on-line fault detection in non-stationary structural systems via a statistical model based method, in: Proceedings of the Second European Workshop on Structural Health Monitoring, Munich, Germany, 2004, pp. 687–694.
[16] Y. Zhan, V. Makis, A.K.S. Jardine, Adaptive state detection of gearboxes under varying load conditions based on parametric modelling, *Mechanical Systems and Signal Processing* 20 (1) (2006) 188–221.
[17] R. Ben Mrad, S.D. Fassois, J.A. Levitt, A polynomial-algebraic method for non-stationary TARMA signal analysis—part II: application to modelling and prediction of power consumption in automobile active suspension systems, *Signal Processing* 65 (1) (1998) 21–38.
[18] R. Ben Mrad, Non-linear systems representation using ARMAX models with time-dependent coefficients, *Mechanical Systems and Signal Processing* 16 (5) (2002) 803–815.
[19] D. Newland, Wavelet analysis of vibration, parts I and II, *Journal of Vibration and Acoustics* 116 (1994) 409–425.
[20] P.D. Spanos, G. Failla, Wavelets: theoretical concepts and vibrations related applications, *The Shock and Vibration Digest* 37 (5) (2005) 359–375.
[21] G.E.P. Box, G.M. Jenkins, G.C. Reinsel, *Time Series Analysis, Forecasting and Control*, third ed., Prentice-Hall, Englewood Cliffs, NJ, 1994.
[22] M. Niedzwiecki, *Identification of Time-Varying Processes*, Wiley, New York, 2000.
[23] Y. Grenier, Parametric time–frequency representations, in: G. Longo, B. Picibono (Eds.), *Time and Frequency Representations of Signals and Systems*, Springer, Berlin, 1989.
[24] J.S. Owen, B.J. Eccles, B.S. Choo, M.A. Woodings, The application of auto-regressive time series modelling for the time–frequency analysis of civil engineering structures, *Engineering Structures* 23 (5) (2001) 521–536.
[25] J.E. Cooper, K. Worden, On the physical parameter estimation with adaptive forgetting factors, *Mechanical Systems and Signal Processing* 14 (5) (2000) 705–730.
[26] W. Gersch, T. Brotherton, Estimation of stationary structural system parameters from non-stationary random vibration data: a locally stationary model method, *Journal of Sound and Vibration* 81 (2) (1982) 215–227.
[27] J.E. Cooper, Identification of time varying modal parameters, *The Aeronautical Journal of the Royal Aeronautical Society* 94 (1990) 271–278.
[28] W. Gersch, G. Kitagawa, A time varying AR coefficient model for modeling and simulating earthquake ground motion, *Earthquake Engineering and Structural Dynamics* 13 (2) (1985) 243–254.
[29] G. Kitagawa, W. Gersch, A smoothness priors time-varying AR coefficient modeling of nonstationary covariance time series, *IEEE Transactions on Automatic Control* 30 (1) (1985) 48–56.
[30] R. Ben Mrad, S.D. Fassois, J.A. Levitt, A polynomial-algebraic method for non-stationary TARMA signal analysis—part I: the method, *Signal Processing* 65 (1) (1998) 1–19.
[31] G.N. Fouskitakis, S.D. Fassois, On the estimation of nonstationary functional series TARMA models: an isomorphic matrix algebra based method, *ASME Journal of Dynamic Systems, Measurements and Control* 123 (4) (2001) 601–610.
[32] F. Kozin, Estimation and modelling of non-stationary time series, in: Proceedings of the Symposium on Computational Methods in Engineering, University of Southern California, 1977, pp. 603–612.

[33] L. Ljung, *System Identification: Theory for the User*, second ed., Prentice-Hall PTR, 1999.
[34] R. Ben Mrad, S.D. Fassois, Recursive identification of vibrating structures from noise-corrupted observations, 1, identification approaches, *ASME Journal of Vibration and Acoustics* 113 (1991) 354–361.
[35] R. Ben Mrad, S.D. Fassois, Recursive identification of vibrating structures from noise–corrupted observations, 2, performance evaluation via numerical and laboratory experiments, *ASME Journal of Vibration and Acoustics* 113 (1991) 362–368.
[36] Y. Grenier, Time-dependent ARMA modeling of nonstationary signals, *IEEE Transactions on Acoustics, Speech, Signal Processing* 31 (4) (1983) 899–911.
[37] M.D. Spiridonakos, S.D. Fassois, FS-TARMA models for non-stationary vibration analysis: an overview and comparison, in: Proceedings of the 15th IFAC Symposium on System Identification, Saint-Malo, France, 2009, pp. 1241–1246.
[38] G.G. Walter, *Wavelets and Other Orthogonal Systems with Applications*, CRC Press, Boca Raton, 1994.
[39] N.R. Draper, H. Smith, *Applied Regression Analysis*, third ed., Wiley, New York, 1998.
[40] S.D. Fassois, MIMO LMS-ARMAX identification of vibrating structures—part I: the method, *Mechanical Systems and Signal Processing* 15 (4) (2001) 723–735.